Diffusion of hydrogen in cubic Laves phase $HfTi_2H_x$

2004 J. Phys.: Condens. Matter 16 8891

(http://iopscience.iop.org/0953-8984/16/49/007)

INSTITUTE OF PHYSICS PUBLISHING JOURNAL OF PHYSICS: CONDENSED MATTER

J. Phys.: Condens. Matter **16** (2004) 8891–8903 PII: S0953-8984(04)79223-1

Diffusion of hydrogen in cubic Laves phase $HfTi_2H_x$

Bhawna Bhatia[1], Xinjun Luo[2], C A Sholl[2] and David S Sholl[1,3]

[1] Department of Chemical Engineering, Carnegie Mellon University, Pittsburgh, PA 15213, USA
[2] Physics and Electronics, University of New England, Armidale, NSW 2351, Australia
[3] National Energy Technology Laboratory, Pittsburgh, PA 15236, USA

E-mail: csholl@metz.une.edu.au

Received 16 April 2004
Published 26 November 2004
Online at stacks.iop.org/JPhysCM/16/8891
doi:10.1088/0953-8984/16/49/007

Abstract

Experimental data for proton nuclear spin relaxation and diffusion of H in $HfTi_2H_x$ are analysed by simultaneously fitting the temperature-dependent relaxation and diffusion data with a common set of parameters. $HfTi_2H_x$ has the C15 structure with the H occupying the inequivalent interstitial e and g sites. The fitting of the relaxation data uses a rigorous theory of nuclear spin relaxation between inequivalent sites and makes no assumptions about which types of H jumps are significant for the relaxation. The diffusion data is fitted by developing the theory of diffusion between the inequivalent e and g interstitial sites, which enables the diffusivity to be calculated rigorously as a function of temperature from the H jump rates in the low concentration limit. Monte Carlo simulations are used to estimate the effect of diffusion correlation effects at higher H concentrations. Models for diffusion between inequivalent sites involve a large number of parameters and density functional theory (DFT) calculations are used to provide constraints on them. Good fits to both the relaxation and diffusion data are obtained for energy parameters that are close to those from the DFT calculations. A complete set of jump parameters for H between the interstitial sites is deduced which provides a detailed microscopic description of the diffusion as a function of temperature.

1. Introduction

The diffusion of hydrogen in the hydrogen-stabilized Laves phase compound C15-$HfTi_2H_x$ has recently been studied by Eberle *et al* (2002) (to be referred to as EMSK). This work involved temperature-dependent measurements of the diffusivity and proton spin-lattice relaxation rates for $x = 3.9$, 4.0 and 4.2. Hydrogen occupies the interstitial e and g sites in this compound with mostly e site occupancy. EMSK analysed the spin-relaxation data in terms of a model of diffusion between e sites, which causes long-range diffusion, and localized jumps between g sites which do not contribute to the diffusivity. Some diffusion parameters obtained by fitting the relaxation data were reasonably consistent with the results of the diffusivity measurements.

$HfTi_2$ is an example of a class of Laves phase intermetallic compounds in which H has several types of jumps with different characteristic frequencies, partly as a result of diffusion between crystallographically inequivalent sites (Skripov 2004). Diffusion between inequivalent sites complicates the analysis of relaxation and diffusion data considerably. The usual approach for analysing relaxation data in these compounds has been to assume particular, and independent, H jump models that are responsible for different features of the relaxation rate behaviour (see for example EMSK). A significant complication that arises with these jump models is that they require assumptions to be made regarding the microscopic mechanism of intersite hopping. The validity of these assumptions is difficult to determine experimentally.

The aim of this paper is to use a more rigorous theoretical basis to analyse the proton spin-relaxation data of $HfTi_2H_x$ as an example of this class of compounds. Our results rely on a combination of two ideas. Firstly, we use a general theory for site hopping in the interstitial sites of the C15-AB_2 structure that makes no assumptions about the relative importance of particular types of hops for determining long-range diffusion. Secondly, we use *ab initio* density functional theory (DFT) calculations to estimate the energy barriers and hopping rates that define the hopping theory. These estimates provide crucial guidance for the refinement of the model parameters by comparison with experimental measurements of diffusion and spin-relaxation. The combination of these two approaches provides a powerful tool for the analysis of hydrogen diffusion in intermetallic compounds.

Our approach is used to provide a consistent description of both spin-relaxation and self-diffusion of H amongst the inequivalent e and g sites of the C15-AB_2 structure. It is known (Jaroszkiewicz and Strange 1985, Sholl 1998) that the magnetization recoveries for spin-relaxation due to diffusion amongst inequivalent sites involves a sum of exponentials. By using the Bloembergen–Purcell–Pound (BPP) model (Bloembergen *et al* 1948) for the spectral density functions, we show how these multiple exponentials provide the experimentally observable results for $HfTi_2H_x$. To examine self-diffusion, we specify the temperature-dependent jump rates between each pair of adjacent sites in the C15-AB_2 structure. We then use the method of Braun and Sholl (1998), which provides a general tool for calculating the diffusivity D for diffusion on an arbitrary set of inequivalent sites with long-range periodicity. This method is valid for low concentrations of the diffusing species, so it does not account for the correlation effects that arise at higher concentrations. These correlation effects can be included by computing D using Monte Carlo simulations, and we will show that these effects are small in the present application.

The relaxation and diffusion theory outlined above can, in principle, be used to fit the available relaxation and diffusion data with a common set of parameters for the elementary jumps in the diffusion model. These parameters and the diffusion theory can then provide a detailed picture of the diffusion of H in these AB_2 compounds. However, our general model of diffusion between e and g sites involves a large number of parameters. This creates a major problem in the fitting of the relaxation and diffusion data because of the complexity of the fitting procedure and because reasonable fits of the data can be obtained for different sets of parameters. To overcome this problem, we have used *ab initio* calculations of the energy differences between sites and the activation energies for each possible jump using DFT. The aim of the DFT calculations is not to provide precise values of the parameters, but rather to provide reasonable estimates that can be used to restrict the ranges of the parameters used in the data fitting. We will show that using DFT results in this manner does indeed provide useful information. By using the DFT-derived model parameters as a starting point for refinement of the model with respect to experimental data, we are able to obtain a model that self-consistently accounts for self diffusion and spin-relaxation experiments and provides new insight into the microscopic mechanism of H diffusion in $HfTi_2H_x$.

The relevant theory of nuclear spin relaxation is described in section 2, and the theory for calculating the diffusivity D for diffusion between inequivalent sites is given in section 3. These sections also define the microscopic parameters that must be determined to describe the system of interest. In section 4, the details of the DFT calculations used to provide initial estimates for these parameters are given. The procedure used to refine these parameters is given in section 5, along with a discussion of the new insights into diffusion in $HfTi_2H_x$ that come out of our model.

2. Nuclear spin relaxation theory

Nuclear spin relaxation due to magnetic dipolar coupling and diffusion of spins on inequivalent sites involves magnetization recoveries that are linear combinations of exponentials (Jaroszkiewicz and Strange 1985, Sholl 1998, Luo and Sholl 2003). For diffusion of H on e and g sites in the cubic C15-AB_2 structure, the components of magnetizations $M_e(t)$ and $M_g(t)$ of protons on the e and g sites are the solutions of

$$\frac{dM_e}{dt} = -a_{ee}M_e - a_{eg}M_g \qquad \text{and} \qquad \frac{dM_g}{dt} = -a_{ge}M_e - a_{gg}M_g, \tag{1}$$

where the time-independent coefficients a_{ee}, a_{eg}, a_{ge} and a_{gg} depend on the spectral density functions of the magnetic dipolar fluctuations and the jump rates between e and g sites.

The expressions for the coefficients for longitudinal relaxation in the laboratory frame, and for spectral density functions averaged over magnetic field directions which is appropriate for polycrystal samples, are

$$a_{ee} = 4\Gamma_{eg}(1 - c_g) + \frac{K}{15}[3J_{ee}(\omega) + 12J_{ee}(2\omega) + J_{eg}(0) + 3J_{eg}(\omega) + 6J_{eg}(2\omega)], \tag{2}$$

$$a_{eg} = -8\Gamma_{ge}(1 - c_e) + \frac{c_e}{3c_g}\frac{K}{15}[-J_{eg}(0) + 6J_{eg}(2\omega)], \tag{3}$$

$$a_{ge} = -4\Gamma_{eg}(1 - c_g) + \frac{3c_g}{c_e}\frac{K}{15}[-J_{ge}(0) + 6J_{ge}(2\omega)], \tag{4}$$

$$a_{gg} = 8\Gamma_{ge}(1 - c_e) + \frac{K}{15}[3J_{gg}(\omega) + 12J_{gg}(2\omega) + J_{ge}(0) + 3J_{ge}(\omega) + 6J_{ge}(2\omega)], \tag{5}$$

where $K = \gamma^4\hbar^2 I(I + 1)$, γ is the gyromagnetic ratio of a spin, I is the quantum number of the spin, $\omega = \gamma B_0$ is the resonant frequency of the spin in the applied magnetic field B_0, and $J_{\alpha\beta}(\omega)$ are spectral density functions which are described below. The first terms on the right-hand sides of these equations correspond to the transfer of magnetization between e and g sites due to the jumps of the spins. The attempted jump rates of the spins are $\Gamma_{\alpha\beta}$ where α and β are e or g, and a jump will be blocked with a probability $(1 - c_\beta)$. There are three nearest neighbour g sites of an e site and one nearest neighbour e site of a g site.

The solution of the differential equations (1) shows that each of $M_e(t)$ and $M_g(t)$ are linear combinations of two exponentials. The observed magnetization is $M(t) = M_e(t) + M_g(t)$ and

$$M(t) = U\exp(-\lambda_+ t) + V\exp(-\lambda_- t), \tag{6}$$

where

$$\lambda_{\pm} = (a_{ee} + a_{gg} \pm f)/2, \tag{7}$$

$$U = [(a_{ee} + a_{ge} - \lambda_{-})M_e(0) + (a_{eg} + a_{gg} - \lambda_{-})M_g(0)]/f, \tag{8}$$

$$V = [(\lambda_{+} - a_{ee} - a_{ge})M_e(0) + (\lambda_{+} - a_{eg} - a_{gg})M_g(0)/f, \tag{9}$$

$$f = [(a_{ee} - a_{gg})^2 + 4a_{eg}a_{ge}]^{1/2}. \tag{10}$$

If the jump rates $\Gamma_{\alpha\beta}$ between the sites are much greater than the spectral density function terms in equations (2)–(5), it can be shown that only the exponential with λ_{-} is observable experimentally and that the expression for this exponent is

$$R_1 = \frac{K}{5}\left\{\frac{4c_e}{x}[J_{ee}(\omega) + 4J_{ee}(2\omega) + J_{eg}(\omega) + 4J_{eg}(2\omega)] + \frac{12c_g}{x}[J_{gg}(\omega) + 4J_{gg}(2\omega) + J_{ge}(\omega) + 4J_{ge}(2\omega)]\right\}. \tag{11}$$

This expression is the same as that obtained by generalizing the relaxation rate for diffusion on equivalent sites to the case of inequivalent sites by simply taking the weighted averages for the various e and g site dipolar interactions. This case of rapid jumps between the inequivalent sites corresponds physically to the establishment of a spin temperature. It will be shown in section 5 that the expression (11) for R_1 is an excellent approximation for λ_{-} in $HfTi_2H_x$.

The spectral density functions $J_{\alpha\beta}(\omega)$ are the Fourier transforms of the correlation functions $G_{\alpha\beta}(t)$ of the magnetic dipolar fluctuations between pairs of diffusing spins. Within the BPP model (Bloembergen *et al* 1948) the time dependence of the correlation function is given by the probability of no jump of either spin of a pair in a time t, which is $e^{-\Gamma t}$, where Γ is the sum of the jump rates of each of the spins. The BPP approximations for the spectral density functions are then (Jaroszkiewicz and Strange 1985, Luo and Sholl 2003) given by

$$J_{ee}(\omega) = 2c_e S_{ee}\frac{2\Gamma_e}{(2\Gamma_e)^2 + \omega^2}, \tag{12}$$

$$J_{eg}(\omega) = 2c_g S_{eg}\frac{\Gamma_e + \Gamma_g}{(\Gamma_e + \Gamma_g)^2 + \omega^2}, \tag{13}$$

$$J_{ge}(\omega) = 2c_e S_{ge}\frac{\Gamma_e + \Gamma_g}{(\Gamma_e + \Gamma_g)^2 + \omega^2}, \tag{14}$$

$$J_{gg}(\omega) = 2c_g S_{gg}\frac{2\Gamma_g}{(2\Gamma_g)^2 + \omega^2}, \tag{15}$$

where Γ_e is the total jump rate from an e site to any site and Γ_g is the total jump rate from a g site to any site. These jump rates are

$$\Gamma_e = 12(1 - c_e)\Gamma_{ee} + 3(1 - c_g)\Gamma_{eg}, \tag{16}$$

$$\Gamma_g = (1 - c_e)\Gamma_{ge} + 2(1 - c_g)\Gamma_{gg1} + (1 - c_g)\Gamma_{gg2}, \tag{17}$$

where Γ_{ee}, Γ_{eg}, Γ_{ge}, Γ_{gg1}, and Γ_{gg2} are the attempted jump rates from an e site to an e site, from an e site to a g site, from a g site to an e site, from a g site to a neighbouring g site within

a hexagon, and from a g site to a neighbouring g site in another hexagon, respectively. The jump rate Γ_{ee} will be omitted in the fitting of the $HfTi_2H_x$ data in section 5 because our DFT calculations show that this rate is negligibly small, but is included here for completeness. The parameters $S_{\alpha\beta}$ are the summations $\sum_i r_i^{-6}$ where the origin is a site of type α and r_i is the distance to sites of type β.

The values of c_e and c_g are related to the jump rates Γ_{eg} and Γ_{ge} by the principle of detailed balance so that

$$c_e(1-c_g)\Gamma_{eg} = c_g(1-c_e)\Gamma_{ge}. \tag{18}$$

Solving this equation and $4c_e + 12c_g = x$ gives c_e as a solution of the quadratic equation

$$4(z-1)c_e^2 - [12 + 4z + x(z-1)]c_e + xz = 0, \tag{19}$$

where $z = \Gamma_{ge}/\Gamma_{eg}$. The values of c_e and c_g are then the positive solutions of this quadratic equation and $c_g = (x - 4c_e)/12$.

3. Diffusion theory

The diffusivity D of atoms diffusing between inequivalent sites can be calculated from the jump rates between sites by the method of Braun and Sholl (1998) for low concentrations of the diffusing species. The components of the diffusivity tensor D_{ij} are calculated from

$$D_{ij} = \mathbf{v}_0^* \mathbf{\Lambda}_1 \mathbf{v}_1 + \mathbf{v}_0^* \mathbf{\Lambda}_2 \mathbf{v}_0/2, \tag{20}$$

where $\mathbf{v}_1$ is the solution of the matrix equation

$$\mathbf{\Lambda}_0 \mathbf{v}_1 = -\mathbf{\Lambda}_1 \mathbf{v}_0. \tag{21}$$

In these expressions $\mathbf{v}_0$ is a one-dimensional matrix determined by the probability of occupation of each type of site, and $\mathbf{\Lambda}_0$, $\mathbf{\Lambda}_1$, and $\mathbf{\Lambda}_2$ are square matrices involving the geometry of the jumps and the jump rates. The size of the matrices is the number of diffusion sites per unit cell. The above equations can be solved analytically in simple cases and numerically when an analytic solution is not possible. For the case of e and g sites in the C15-AB_2 structure, there are 128 sites per cubic unit cell. This can be reduced to 32 by choosing a non-cubic primitive FCC unit cell, but the set of linear equations (21) is still too large for an algebraic solution. A numerical solution is therefore necessary in this case. The diffusivity tensor is isotropic for this structure.

The above discussion is for diffusion in the low-concentration limit. The results are, however, also likely to be a good approximation at concentrations of $x \sim 4$ in $HfTi_2H_x$ provided that the jump rates used in the calculations are the actual jump rates including site-blocking effects rather than attempted jump rates. This is because the values of the correlation factors that take account of the correlations at higher concentrations are likely to be close to unity because the g site concentration is expected to be quite low. The effect of the correlations can be estimated by performing Monte Carlo simulations of the diffusivity and the results of these calculations are given in section 5.

The theory in this and the previous section enables the spin relaxation rates and the diffusivity to be calculated from a set of jump rates Γ_{ee}, Γ_{eg}, Γ_{ge}, Γ_{gg1} and Γ_{gg2}. If each jump is assumed to have an Arrhenius form, then five prefactors and five activation energies must be determined if these jump rates are to be fitted to experimental data. Estimates of their values are therefore very useful in constraining the ranges of the parameters to be used in data-fitting procedures. The following section describes DFT calculations to provide these estimates. The data-fitting procedure is then described in section 5.

4. Density functional theory calculations

It has been recognized for many years that the diffusion of light interstitials in metals can show significant quantum effects, especially at low temperatures (Flynn 1972). A first-principles calculation of the diffusion rate of H in metals is a difficult task if quantum effects such as the appearance of resonant modes are to be included accurately (Schober and Stoneham 1988, Stoneham 1990). Our aim here is not to provide precise values of the individual jump rates, but rather to constrain the range of parameters used in the data fitting in the following section. Simpler DFT calculations that do not include full quantum effects have therefore been used. Plane wave DFT calculations have provided a useful computational tool for making quantitative predictions regarding the binding, vibration and diffusion of H in interstitial sites in pure metals (Smithson *et al* 2002) and disordered alloys (Kamakoti and Sholl 2003), as well as on metal surfaces (Greeley and Mavrikakis 2003, Jiang and Carter 2003). DFT has also been used by Hong and Fu (2002) to examine H binding in e and g sites of a series of C15-AB_2 materials with A = Zr. To our knowledge, DFT has not previously been used to examine H diffusion in C15 intermetallics.

The plane wave DFT calculations to examine H diffusion in $HfTi_2H_x$ were performed using the Vienna *ab initio* simulation package (VASP) (Kresse and Furthmuller 1996) using the supplied ultrasoft pseudopotentials and the PW91-GGA exchange-correlation functional. A computational cell extended by periodic boundary conditions was used to describe a material of infinite extent. The cubic computational cell of $HfTi_2$ comprised 8 Hf and 16 Ti atoms. k-space was sampled using $3 \times 3 \times 3$ k-points positioned using the Monkhorst–Pack scheme. Results using larger numbers of k-points gave very minor total energy differences from calculations with $3 \times 3 \times 3$ k-points. A cutoff energy of 270 eV was used throughout. Geometries were optimized until the forces on all unconstrained atoms were less than 0.03 eV $Å^{-1}$. Unless otherwise specified, all atoms were allowed to relax during geometry optimizations.

Calculations were first performed for $HfTi_2H_x$ with $x = 0$ and 0.125, that is, with 0 and 1 H atom in the computational cell. The initial configuration with $x = 0.125$ had the H atom in an e site of the metal lattice. The results indicated that the C15 crystal structure of $HfTi_2$ is not stable at these loadings; large structural distortions were observed during geometry optimization that significantly disrupted the initial C15 structure. These observations are in agreement with experimental findings that C15-$HfTi_2$ is only stabilized by appreciable loadings of H (EMSK, Skripov *et al* 2000).

The remainder of the calculations were performed for $HfTi_2H_x$ with $x = 4$, and 4.125 (that is, 32 and 33 H atoms in the computational cell). The C15 crystal structure is known experimentally to be stable at these H loadings and our calculations also exhibit this property. For $x = 4$, with H atoms occupying all e sites, the calculations predict a lattice parameter of $a_0 = 8.10$ Å, in excellent agreement with the experimentally reported 8.095 ± 0.005 Å (EMSK). In all subsequent calculations, the lattice parameter was fixed at the DFT-optimized value. In the optimized $HfTi_2H_4$ structure, the Hf–H distance was 1.995 Å and the Ti–H distance was 1.895 Å.

The energy difference between H occupation of e and g sites was determined by moving one of the 32 H atoms in the $HfTi_2H_4$ structure (referred to below as the mobile H atom) from an e site to a g site while keeping the other 31 H atoms at e sites. Geometry optimization of this configuration gives the energy change in moving from an e site to a g site, which we will denote as E_g, to be 0.05 eV. The Hf–H distance for the H atom occupying a g site in this configuration is 2.035 Å and the Ti–H distance is 1.935 Å. Since zero-point energies for interstitial H can be substantial, zero-point energies for the mobile H atom were calculated by determining the vibrational frequencies of the mobile atom in the e and g sites while holding all

other atoms in the computational cell fixed (Kamakoti and Sholl 2003). This approach treats hydrogen vibrations as being decoupled from phonon modes of the crystal. This is clearly a simplification of true vibrational dynamics, but provides an avenue to estimate the interstitial zero-point energies using reasonable amounts of computing resources. This approach has been shown to provide accurate predictions of H vibrational frequencies on metal surfaces (Greeley and Mavrikakis 2003). The e (g) site zero-point energy computed in this way was 0.24 (0.21) eV. Incorporating these zero-point energies in the calculation of E_g gives $E_g = 0.02$ eV. The calculation of the zero-point energies has neglected lattice relaxation which would reduce their magnitudes, but the above results provide a sufficient estimate of E_g for the present purposes.

Transition states for hopping of H between adjacent interstitial sites were determined using the nudged elastic band (NEB) method (Henkelman *et al* 2000). All atoms were allowed to relax during these calculations. Following convergence of the NEB calculations, the configuration most closely approximating a transition state on the computed minimum energy path was geometry optimized using a quasi-Newton algorithm that converges to critical points on the potential energy surface for starting points sufficiently close to a critical point. This procedure allowed the precise location of the transition states. At each transition state, the vibrational frequencies for the mobile H atoms were computed as described above, yielding two real and one imaginary frequencies.

The activation energy for e to g hops was determined by moving one of the 32 H atoms in the $HfTi_2H_4$ structure from an e site to a g site while keeping the other 31 H atoms at e sites. The resulting transition state was 0.22 eV higher in energy than the e site. For g to g hops the optimized geometry with 33 H atoms in the $HfTi_2H_{4.125}$ structure was used, with 32 H at the e sites and the remaining H allowed to move between two g sites. Separate NEB calculations were performed to compute both inter-hexagonal and intra-hexagonal g to g hops. The activation energy for intra-hexagonal hops was found to be 0.07 eV, while the barrier for inter-hexagonal hops was 0.22 eV.

NEB calculations were also used to examine H hops between e sites. In addition to the e to e hops via g sites, e to e hops can take place in principle via the tetrahedral b site, which in the C15-AB_2 structure is defined by four B atoms. The DFT calculations of Hong and Fu (2002) indicated that b sites are extremely unfavourable in a series of C15 intermetallics where A is Zr. The NEB calculations here show that b sites are also extremely unfavorable in $HfTi_2$, with the transition state for e to b hopping lying approximately 1 eV higher in energy than the e site. In comparing this energy to the much lower barriers found above for hopping between e and g sites, it is clear that e to e hops via b sites do not play any significant role in H diffusion in $HfTi_2H_x$.

Once the energy barriers E_a for hops between adjacent sites are known, a simple estimate of the hopping rates Γ between these sites is the Vineyard expression from classical harmonic transition state theory

$$\Gamma = \frac{\nu_1 \nu_2 \nu_3}{\nu_1^{\ddagger} \nu_2^{\ddagger}} e^{-E_a/kT}, \tag{22}$$

where $\nu_i(\nu_j^{\ddagger})$ are the real frequencies associated with the vibrational frequencies of the mobile H atom in the binding site (at the transition state). Estimating the prefactors for site to site hopping in this way gives $2.7 \times 10^{13}\ s^{-1}$ for e to g hops, $1.9 \times 10^{13}\ s^{-1}$ for g to e hops, $1.6 \times 10^{13}\ s^{-1}$ for g to g intra-hexagon hops, and $1.1 \times 10^{13}\ s^{-1}$ for g to g inter-hexagon hops.

The activation energies and hopping rates described above are based upon classical transition state theory. The quantum effect of the zero-point energies can be incorporated into harmonic transition state theory by treating both the binding site and transition state as

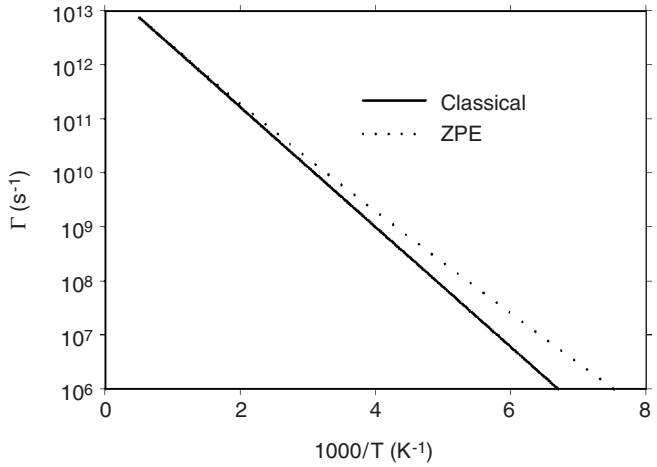

Figure 1. The hopping rate Γ as a function of 1000/T for e to g hops. The classical result is from equation (22), the inclusion of zero-point energy effects is from equation (23).

quantum mechanical harmonic oscillators. The resulting expression is

$$\Gamma = \frac{\nu_1\nu_2\nu_3}{\nu_1^{\ddagger}\nu_2^{\ddagger}} e^{-E_a/kT} \frac{\prod_i \sinh(X_i)/X_i}{\prod_i \sinh(X_i^{\ddagger})/X_i^{\ddagger}}, \tag{23}$$

where $X_i = \hbar\omega_i/(2kT)$, and the products in the numerator (denominator) are over the vibrational frequencies of the mobile atom at the energy minimum (transition state). At low temperatures, the effective activation energy from this expression approaches the difference between the zero-point corrected energy at the minimum and transition state. In this limit, the activation energy for e to g hops is 0.17 eV, while the intra- and inter-hexagonal g to g hops have activation energies of 0.05 and 0.23 eV, respectively. The temperature dependence of the e to g hopping rate as defined in equation (23) is compared to the classical result, equation (22), in figure 1.

5. Fitting of Hf Ti_2H_x relaxation and diffusion data

The aim in this section is to use the theory of the previous three sections to find a set of diffusion parameters to fit both the diffusion data and nuclear spin relaxation data of EMSK for Hf Ti_2H_x with $x = 3.9$, 4.0 and 4.2. The energy of an e site is taken as zero, the energy of a g site is E_g, the height of the energy barrier between the e and g sites is E_{eg}, and the corresponding heights of the energy barriers between g sites are E_{gg1} and E_{gg2} for diffusion between sites on a hexagon and sites between hexagons, respectively. The jump rates are then assumed to be of the Arrhenius forms

$$\Gamma_{eg} = \Gamma_{0eg} \exp(-E_{eg}/kT), \tag{24}$$

$$\Gamma_{ge} = \Gamma_{0ge} \exp(-(E_{eg} - E_g)/kT), \tag{25}$$

$$\Gamma_{gg1} = \Gamma_{0gg1} \exp(-(E_{gg1} - E_g)/kT), \tag{26}$$

$$\Gamma_{gg2} = \Gamma_{0gg2} \exp(-(E_{gg2} - E_g)/kT). \tag{27}$$

Jumps between neighbouring e sites are not included in the diffusion model ($\Gamma_{ee} = 0$) because the DFT calculations showed these jumps to be very unfavourable.

The spin relaxation data are shown in figure 2 for $x = 4.0$ and resonance frequencies of 37.3, 67.7 and 90.0 MHz. The data include the small electronic relaxation contribution (EMSK). The plots show maxima with different slopes on each side of the maxima. EMSK fitted the data (after subtracting the electronic relaxation) with a model that was the sum of two contributions. One of these corresponded to diffusion between the e sites and this was the dominant contribution in the vicinity of a maximum. The other term was attributed to diffusion between g sites within hexagons and this contribution was a broader and lower peak which had its maximum at lower temperatures than the temperature of the experimental maximum. It is useful to analyse the theory of section 3 in terms of such contributions. This can be done for the expression (11) for the relaxation rate R_1. It was verified numerically that this approximation agrees very well with the more rigorous expression for λ_- for the range of diffusion parameters relevant to $HfTi_2H_x$.

The expression (11) can be written within the BPP approximation in the form

$$R_1 = \frac{8K}{5x\omega}\left[c_e^2 S_{ee} F(y_e) + 3c_g^2 S_{gg} F(y_g) + 6c_e c_g S_{ge} F(y_{eg})\right], \tag{28}$$

where $y_e = \omega/(2\Gamma_e)$, $y_g = \omega/(2\Gamma_g)$, $y_{eg} = \omega/(\Gamma_e + \Gamma_g)$ and the function $F(y)$ is

$$F(y) = \frac{y}{1+y^2} + \frac{4y}{1+4y^2}. \tag{29}$$

The function $F(y)$ has a maximum of 1.43 at $y = 0.62$. The expression for R_1 is therefore the sum of three such terms arising from magnetic dipolar interactions between pairs of protons initially on e sites (the ee term), between protons initially on g sites (the gg term), and between protons with initially one on an e site and one on a g site (the eg term), respectively. Each of these terms will contribute a curve with a maximum, where the magnitude and the position of the maxima will be different for each term.

The values of the sums $S_{\alpha\beta}$ for the ideal e and g site positions in the C15-AB_2 structure are, in units of a_0^{-6} where a_0 is the lattice parameter, $S_{ee} = 7.40 \times 10^3$, $S_{eg} = 3S_{ge} = 2.87 \times 10^5$, $S_{gg} = 2.23 \times 10^5$. The lattice parameter is $a_0 = 8.095$ Å. The sums could be different from these ideal values because H do not occupy the ideal positions in $HfTi_2H_x$ (EMSK) and because the minimum H–H separation in metal–hydrogen systems is 2.1 Å according to the Westlake criterion (see, for example, Flanagan and Oates 1988). For the ideal e and g positions in $HfTi_2H_x$ the distance between neighbouring g sites within a hexagon, and between neighbouring e and g sites, is 1.23 Å. The distance between neighbouring g sites on adjacent hexagons is 1.47 Å. It is therefore unlikely that such pairs of sites would both be occupied by H. This exclusion effect would reduce the values of the sums S_{eg}, S_{ge} and S_{gg} substantially since it is the nearest neighbours that dominate the sums. Three further parameters were introduced to account for these effects: a factor f_1 that multiplies S_{ee}, a factor f_2 that multiplies S_{eg} and S_{ge}, and a factor f_3 that multiplies S_{gg}. From the above discussion it would be expected that the values of f_2 and f_3 would be appreciably less than unity, and that $f_1 \sim 1$ since the distance between neighbouring e sites is 2.86 Å and occupation of these sites would not be limited by the Westlake criterion.

The ratios of the maxima of the ee, gg and eg terms in equation (28) can then be estimated and they are $f_1 : 91 f_3 (c_g/c_e)^2 : 78 f_2 (c_g/c_e)$. Since the g site occupation probability in $HfTi_2H_x$ is small, the ratio c_g/c_e will be appreciably less than unity. The above reasoning suggests that the ee term in equation (28) is dominant near the main peak in the data, that the gg term is likely to be small, and that the eg term contributes a lower peak at a temperature

different from that at which the main peak occurs. Further evidence that the ee term is dominant near the main peak is that the value of the maximum due to this term is $27 f_1 c_e^2$ for $x = 4$ and a frequency of 37.3 MHz. This is quite close to the experimental maximum of 25.4 s^{-1} for c_e and $f_1 \sim 1$. Since the ee term dominates near this maximum, the position of the maximum is at a temperature for which $\omega/(2\Gamma_e) = 0.62$. This relation can be used to determine one of the diffusion parameters by fitting the position of the relaxation maximum.

A least-squares fit of the relaxation data (after subtraction of the electronic relaxation contribution) was therefore undertaken by omitting the gg term in equation (28) and varying the energy parameters in ranges about the values obtained from the DFT calculations. The jump rate prefactors from the DFT calculations were not used in the fitting procedure and their values were taken as free parameters. The parameter f_3 was not used in the fitting because the gg term is omitted. The jump rate Γ_{gg2} was also taken as zero because the DFT calculations showed that $\Gamma_{gg1} \gg \Gamma_{gg2}$ in general. The number of independent trial parameters was reduced by fitting the value and temperature of the peak in the experimental data, and by fitting the value and temperature of one other experimental point in each calculation of the variance for each set of trial parameters. The values of some of the parameters are also related by the principle of detailed balance. In addition, one of the fitting parameters was replaced by the value of c_g at 300 K, since $c_g(300\,\mathrm{K})$ is expected to be approximately 0.05–0.07 (EMSK). The value of $c_g(300\,\mathrm{K})$ was varied around this range. Excellent fits of the relaxation data were obtained by this procedure. The diffusivity D was then calculated as a function of temperature, using the methods described in section 3, for the parameters obtained from the fits to the relaxation data. The resulting values of D were significantly smaller than the experimental values. This set of parameters from the fits to the relaxation data were therefore unsatisfactory. A further least-squares fit of the relaxation data was therefore undertaken with an additional constraint that the resulting values of the diffusivity were close to the experimental values for each trial set of parameters. In addition, including Γ_{gg2} in the fits gave a significant change to the values of D but had a negligible effect on the relaxation rates. A set of parameters was then sought which would give a low value of the variance in the relaxation fit and also a reasonable fit to the diffusion data. When such a set of parameters was found, the relaxation rate was recalculated including the gg term in equation (28) to ensure this produced a negligible effect.

The results for the simultaneous fits of the relaxation and diffusion data are shown in figures 2 and 3 for $x = 4.0$. Similar quality of fits (not shown) were obtained for $x = 3.9$ and 4.2. The ee and eg contributions to the relaxation rates for the 37.3 MHz data are also shown in figure 2. The values of the diffusivity calculated by equations (20) and (21) are shown in figure 3. Monte Carlo calculations of the diffusivity were carried out for the same parameters as those used in figure 3 to investigate the effects of correlations in the diffusion that are neglected in the low-concentration-limit theories of equations (20) and (21). These correlations are those that occur between jumps of a particular H and the motions of other H atoms at non-vanishing values of concentration x. The Monte Carlo results agreed with the results of the exact low-concentration results in figure 3 to within ~10% over the range of temperatures shown, so that the correlation effects are not significant within the accuracy of the fitting procedures. This result is consistent with the fact that for $x \sim 4$ most e sites are occupied and most g sites unoccupied. Since the long range diffusion proceeds via the g sites the correlation effects would not be expected to be significant.

The parameters for these fits and the values from the DFT calculations are given in table 1. The quality of the fits is quite sensitive to small changes in the energies and so the energy parameters are given to a precision of 0.001 eV. The accuracy of the energies is not, however, of this precision because other combinations of parameters with less precision can also produce comparable fits. Since there is no discernible trend in the parameters as a function of

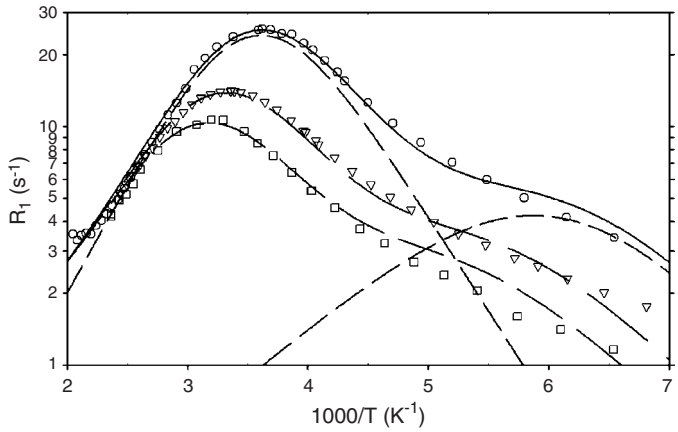

Figure 2. Fit of the relaxation data for $x = 4.0$. Symbols are experimental data: ○, 37.3 MHz; △, 67.7 MHz; and □, 90.0 MHz. The continuous lines are the fit to the data (including the electronic relaxation contribution). The dashed lines are the ee contribution (left-hand side peak) and the eg contribution (right-hand side peak) to the relaxation rate given by equation (28) for the 37.3 MHz data.

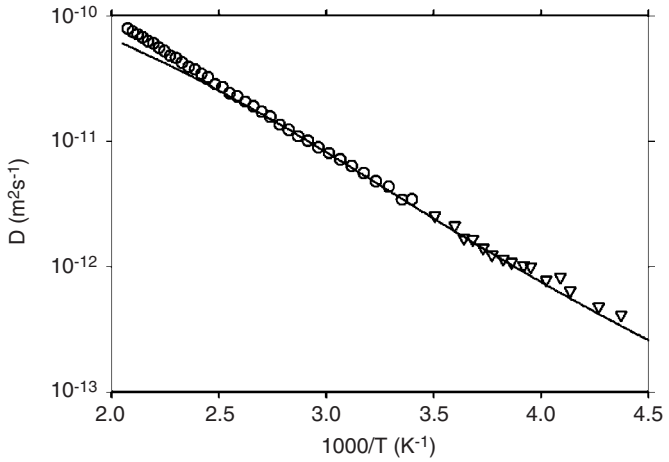

Figure 3. Fit to the diffusivity data for $x = 4.0$ for the same parameters as in figure 2. The symbols are the experimental data. The solid line is the calculated D using equations (20) and (21).

concentration x the differences between the values of the parameters for different x is possibly an indication of their accuracy. The energies deduced from the fits are in reasonable agreement with the estimates from the DFT calculations. The values of the prefactors Γ_{0gg2} are also in reasonable agreement with the DFT calculations, but the other prefactors are significantly smaller than the DFT results. If the diffusivity is calculated directly from the DFT parameters, the results for D on an Arrhenius plot show that the slope is in reasonable agreement with experiment, but the absolute values of D are too large. This suggests that the approximations in our DFT calculations lead to an overestimate of the prefactors in this system.

The values of $f_1 \sim 1.5$ and $f_2 \sim 0.04$ suggest that H does not occupy the ideal positions of the interstitial e and g sites. Small changes in the positions of the sites can cause significant

Table 1. Values of the parameters for the fits of the theory to the relaxation and diffusion data for $x = 3.9$, 4.0 and 4.2. DFT (classical) are the results of the DFT calculations for classical transition rate theory and DFT (ZPE) are the energies calculated by including zero-point-energy corrections. Energies are in eV and prefactors are in units of s^{-1}.

	$x = 3.9$	$x = 4.0$	$x = 4.2$	DFT (classical)	DFT (ZPE)
E_g	0.059	0.048	0.057	0.05	0.02
E_{eg}	0.155	0.166	0.163	0.22	0.17
$E_{gg1} - E_g$	0.078	0.090	0.091	0.07	0.05
$E_{gg2} - E_g$	0.28	0.28	0.28	0.22	0.23
Γ_{0eg}	4.5×10^{10}	6.6×10^{10}	6.5×10^{10}	2.7×10^{13}	
Γ_{0ge}	1.5×10^{11}	3.0×10^{11}	2.7×10^{11}	1.9×10^{13}	
Γ_{0gg1}	6.0×10^{10}	1.1×10^{11}	1.2×10^{11}	1.6×10^{13}	
Γ_{0gg2}	2.7×10^{13}	3.3×10^{13}	3.9×10^{13}	1.1×10^{13}	
f_1	1.49	1.58	1.45		
f_2	0.040	0.032	0.038		
c_g(300 K)	0.080	0.088	0.089		

changes to the values of the lattice sums $S_{\alpha\beta}$ because of the $1/r^6$ summand. The small value of f_2 also suggests that the H are excluded from near-neighbour positions on the interstitial sites because of the Westlake criterion. The values of c_g at 300 K in table 1 are in reasonable agreement with the values of 0.05–0.07 deduced from neutron scattering experiments on the deuterides (EMSK).

The model used by EMSK to analyse the relaxation data involved the sum of two independent terms. One of these was diffusion between e sites which produces long-range diffusion. Since direct ee hops are energetically unfavourable, the diffusion between e sites must proceed via g sites which is strictly inconsistent with the model used for the spectral density functions. The present results do, however, agree with the EMSK model in that it is the ee magnetic dipolar interactions that dominate the relaxation near the peak in the relaxation rates. The second term used by EMSK was relaxation due to dipolar interactions between H fixed at e sites with H undergoing localized motion within hexagons formed by six g sites. The present theory also deduces that these eg interactions produce a significant contribution to the relaxation rates at lower temperatures. This theory, however, includes all eg, ge and gg hops within the BPP approximation compared with just the gg hops within hexagons used by EMSK for the eg interactions.

The values of a complete set of parameters for jumps between the e and g sites enables the nature of diffusion of H in $HfTi_2H_x$ to be investigated in detail. The various jump rates between interstitial sites and the fractions of H on e and g sites were calculated as functions of temperature. The following conclusions are valid for all temperatures such that $1000/T > 2$. Most of the H occupies e sites and following a jump from an e to a g site, the H is more likely to jump to another g site than return to the e site because the jump rates to g sites are faster than the jump rate to an e site. This effect becomes more pronounced as the temperature decreases. The jumps from one g site to another are mainly between hexagons at high temperatures, but change to jumps mainly within hexagons with decreasing temperature. At low temperatures the jumps within hexagons greatly dominate. For example, for $1000/T = 7$ the gg1 jump rate within hexagons is $\sim 10^5$ faster than the gg2 jump rate between hexagons. The physical picture of the diffusion is therefore that of H jumping from an e to a g site and then diffusing between g sites before returning temporarily to another e site. At low temperatures, very rapid diffusion within a particular hexagon of g sites will occur before a jump to another hexagon or e site. This physical picture is in general agreement with the diffusion model used by EMSK.

6. Conclusions

The combination of nuclear spin relaxation data, diffusion data, DFT calculations, and the theory of diffusion and relaxation for H hopping between inequivalent sites has been used to analyse diffusion of H in $HfTi_2H_x$. The theory of diffusion between inequivalent sites produces a much larger set of parameters than is the case for diffusion between equivalent sites. Fitting these parameters to the relaxation data alone does not generate unique values of the parameters and the DFT estimates of the diffusion parameters are extremely useful in providing constraints on them. The combination of the relaxation and diffusion data is also valuable in providing further constraints.

A good fit to both the relaxation and diffusion data was obtained for a set of activation energies that are close to the DFT values. The jump frequency prefactors from the fit are substantially smaller than the DFT results in general, possibly due to the neglect of a full quantum treatment of the diffusion. Nevertheless, the DFT calculations and methods of analysis used in fitting the diffusion and relaxation data should be generally applicable to diffusion in other Laves phase compounds and in other systems with diffusion between inequivalent sites.

Acknowledgments

BB and DSS received partial support from the DOE University Coal Research Program and the ACS Petroleum Research Fund. DSS also received support from the Camille-Dreyfus Teacher-Scholar program.

References

Bloembergen N, Purcell E M and Pound R V 1948 *Phys. Rev.* **73** 679
Braun O M and Sholl C A 1998 *Phys. Rev.* B **58** 14870
Eberle U, Majer G, Skripov A V and Kozhanov V N 2002 *J. Phys.: Condens. Matter* **14** 153
Flanagan T B and Oates W A 1988 *Topics in Appl. Phys.* **63** 49
Flynn C P 1972 *Defects and Diffusion in Solids* (London: Oxford University Press)
Greeley J and Mavrikakis M 2003 *Surf. Sci.* **540** 215
Henkelman G, Uberuaga B P and Jonsson G 2000 *J. Chem. Phys.* **113** 9901
Hong S and Fu C L 2002 *Phys. Rev.* B **66** 094109
Jaroszkiewicz G A and Strange J H 1985 *J. Phys.: Condens. Matter* **18** 2331
Jiang D E and Carter E A 2003 *Surf. Sci.* **547** 85
Kamakoti P and Sholl D S 2003 *J. Membrane Sci.* **225** 145
Kresse G and Furthmuller J 1996 *J. Comput. Mat. Sci.* **6** 15
Luo X and Sholl C A 2003 *J. Phys.: Condens. Matter* **15** 937
Schober H R and Stoneham A M 1988 *Phys. Rev. Lett.* **60** 2307
Sholl C A 1998 *J. Phys.: Condens. Matter* **10** 3255
Skripov A V 2004 *Defect Diffusion Forum* **224–5** 75
Skripov A V, Combet J, Grimm H, Hempelmann R and Kozhanov V N 2000 *J. Phys.: Condens. Matter* **12** 3313
Smithson H, Marianetti C A, Morgan D, Van der Ven A, Predith A and Ceder G 2002 *Phys. Rev.* B **66** 144107
Stoneham A M 1990 *J. Chem. Soc. Faraday Trans.* **86** 1215